*Tectonophysics*, 182 (1990) 279–300
Elsevier Science Publishers B.V., Amsterdam



# Joint analyses of calcite twins and fault slips as a key for deciphering polyphase tectonics: Burgundy as a case study

O. Lacombe [1], J. Angelier [1], Ph. Laurent [2], F. Bergerat [1] and Ch. Tourneret [2]

[1] *Laboratoire de Tectonique Quantitative, Département de Géotectonique, U.R.A. 1315 C.N.R.S., Université P. et M. Curie, Paris (France)*

[2] *Laboratoire de Tectonique et Géochronologie, U.R.A. 1371 C.N.R.S., Université des Sciences et Techniques du Languedoc, Montpellier (France)*

(Received October 23, 1989; revised version accepted March 5, 1990)

ABSTRACT

Lacombe, O., Angelier, J., Laurent, Ph., Bergerat, F. and Tourneret, Ch., 1990. Joint analyses of calcite twins and fault slips as a key for deciphering polyphase tectonics: Burgundy as a case study. *Tectonophysics*, 182: 279–300.

Determination of regional paleostresses based on calcite twin analysis has been successfully applied for the first time in the Burgundy platform, France. Paleostress tensors obtained with this method are internally consistent along the profile studied. Moreover, the same directions of paleostresses are independently inferred from fault striation analysis.

The results clearly show that the late Mesozoic–Cenozoic evolution of the area has involved polyphase deformation, including (1) NNE–SSW extension, probably late Mesozoic in age, (2) N–S compression related to a major orogenic event in the Pyrenees and Provence, late Eocene in age, (3) E–W extension related to the Oligocene rifting event (the Rhine–Saône rift system), and (4) WNW–ESE compression related to the Late Miocene westward thrusting of Jura.

Calcite twin and striated fault analyses are two complementary tools for paleostress determination: their combined application will allow accurate mapping of paleostress trajectories in intraplate tectonics setting. Moreover, calcite twins can allow stress and paleostress determination when macroscopic features are not observable, which is often the case in very weakly deformed areas and in drill holes.

## Introduction

During the past ten years, several methods of paleostress reconstruction using fault slip data sets have been improved following the first successful attempt by Carey and Brunier (1974): Armijo and Cisternas (1978), Etchecopar et al. (1981), Angelier and Goguel (1979) and Angelier (1984, 1989). These methods have been applied at the regional scale (e.g., Letouzey, 1986), especially in the European platform (Bergerat, 1985, 1987). At the same time, specific methods for analysing calcite tectonic twins in order to reconstruct paleostress tensors have been improved by Laurent et al. (1981, 1990), Laurent (1984) and Etchecopar (1984).

First applications to small areas in the Quercy (Laurent et al., 1990; Tourneret and Laurent, 1990) or in the southern Rhinegraben (Larroque and Laurent, 1988) have been carried out, and suggest that the method proposed by Etchecopar (1984) is suitable for the study of polyphase tectonics based on calcite twin analysis. The purpose of this study is to demonstrate that results provided by calcite twin analysis are valid and consistent at a regional scale, and that combining fault slip and calcite twin studies provides at the present time the most reliable way to reconstruct paleostress trajectories in a platform tectonics setting.

The area investigated is located on the northeastern side of the Bresse graben (also called the Saône graben), along a profile from the Jura "Avant-Monts" (the outermost units of the Jura mountains) to the southeastern portion of the Paris Basin. This profile crosses the transition zone between the Saône graben and the

0040-1951/90/$03.50 

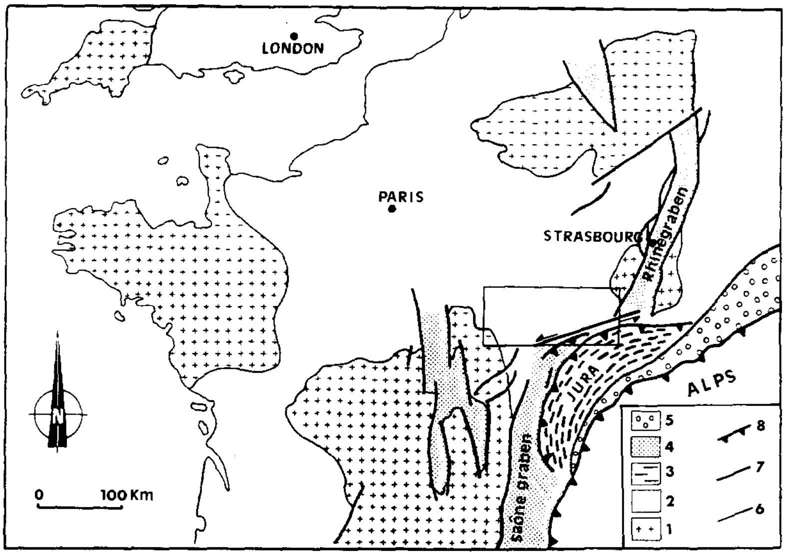


Fig. 1. Schematic map of the West European platform. The frame shows the location of the area studied. *1* = Hercynian basement; *2* = sedimentary formations; *3* = fold-and-thrust" system of Jura (fold axes as dashed lines); *4* = Oligocene rifts; *5* = Miocene molassic basin; *6* = stratigraphic contact; *7* = main faults; *8* = thrust (barbs on upthrust side).

Rhinegraben (Bergerat, 1977) (Fig. 1). Along this profile, six sites have been systematically examined, which are, from south to north, Taxenne, Montagney, Champlitte, Prauthoy, St. Geosmes and Chaumont (Fig. 2).

This geological setting is very appropriate for

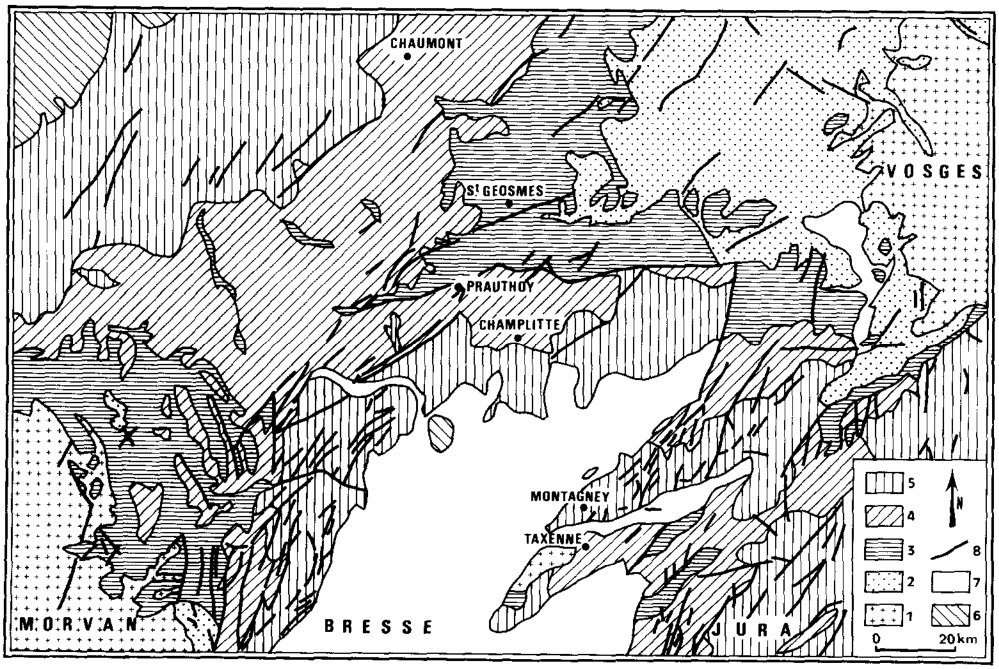


Fig. 2. Geological map of the area studied. Black dots indicate the data collection sites (from south to north), Taxenne, Montagney, Champlitte, Prauthoy, St Geosmes and Chaumont. *1* = Hercynian basement; *2* = Triassic; *3* = Lower Jurassic limestones; *4* = Middle Jurassic limestones; *5* = Upper Jurassic limestones; *6* = Cretaceous; *7* = Cenozoic formations; *8* = main faults.

such a study, because: (1) numerous quarries provide fresh outcrops of limestones, so that large sets of striated faults could be collected and rocks suitable for microscopic analysis could be sampled; and (2) these sites are located in a well-defined geodynamic context, close to major tectonic features which belong to the West European Rift, and the fold-and-thrust system of the Jura (Figs. 1 and 2). Thus, a study of polyphase tectonics can be carried out in good conditions. In numerous outcrops, the Mesozoic formations have been affected by strike-slip and normal faulting. In all cases, sites of data collection display macroscopic evidence of polyphase tectonics, so that the identification of successive events requires cluster analysis and data separation.

Rock formations are limestones, middle to late Jurassic in age (Bathonian to Oxfordian), with abundant interstitial calcite and fossil calcitic infills. These formations have remained horizontal, except close to the Jura folds and thrusts (in the case of Taxenne, the southernmost site).

Calcite twin analysis has been applied to samples from the same sites where fault slip data were collected. In addition, tectonic features such as stylolites and tension gashes have been systematically examined and compared with results of fault slip analysis. It is important to note that the paleostress tensors based on fault slip study and those based on calcite twin analysis have been computed independently.

## Methods for reconstructing paleostresses

### *Microscopic scale: calcite twin analysis*

The *e* twinning process in calcite crystals has been well documented in previous papers, so that there is no need to describe it in detail again (Handin and Griggs, 1951; Turner et al., 1954; Friedman, 1964). It consists of an intracrystalline deformation that affects calcite crystals in a low-temperature plasticity domain. This mechanical twinning occurs with a change of form of the crystal by an approximation to simple shear in a particular sense and direction on a given crystallographic plane (Tullis, 1980; Laurent, 1984) (Fig. 3). The resulting twinned portion of the crystal bears a mirrored crystallographic orientation to the untwinned portion across the twin plane. The twin is consequently easily identifiable by examination in a polarizing microscope (Figs. 4 and 5). Limestones which contain abundant sparitic calcite crystals with random spatial orientation thus allow the development of very numerous mechanical twins. In contrast, in fault tectonics, the fault plane is often imposed in the rock (i.e. inherited surfaces) as for calcite twins, but the slip direction and sense are free (and thus depend only on the stress state).

Experiments on carbonate rocks (Tullis, 1980) have pointed out that: (1) twinning seems to be quite independent of temperature, water and confining pressures, and deformation rate (as a consequence, the normal stress has little or no effect on twinning (Fig. 6) and can be neglected); and (2) twinning is possible provided that the resolved shear stress (the shear stress projected on the twinning direction) exceeds a critical value, the "twinning threshold" of about 10 MPa. The existence and the significance of this critical shear stress for mechanical twinning, as well as its constant value, have been discussed in Cahn (1964), Tullis (1980) and Laurent (1984).

In order to accurately deduce stresses, it is necessary to assume that (1) the crystallographic orientation of the studied sample is random (this point is easily checked through an analysis of the

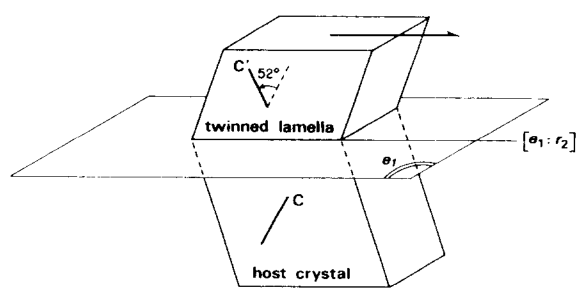


Fig. 3. Schematic sketch of a twin lamella in a calcite crystal. Twin plane (i.e. composition plane) horizontal, referred to as $e_1$. $C$, $C'$ = optical axes of the host grain and of the twinned lamella, respectively (the plane containing $C$ and $C'$ is perpendicular to $e_1$). The twinning direction [$e_1$ : $e_2$] is the direction of motion of the atoms located above the twin plane. The sense of shear is indicated by an arrow (and imposed by crystal network orientation).

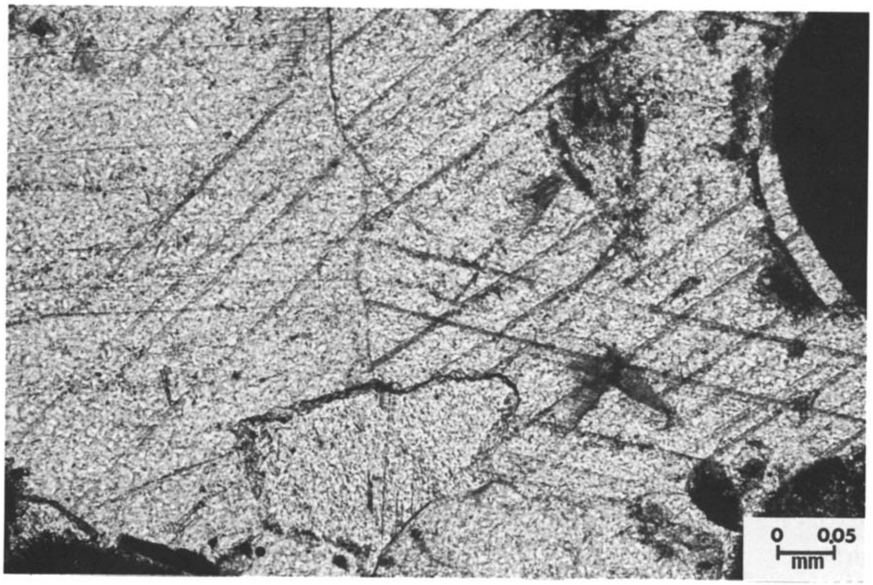


Fig. 4. Thin section (in natural light) of a limestone collected in Burgundy. Twin lamellae appear generally as sharply defined straight lines which cross-cut the host crystal. The two sets of twin lamellae observable here are oblique at large angles to the thin section and thus appear as thin straight lines.

stereographic projection of the *c* axes and of poles of twinned and untwinned *e* planes as in Fig. 7; the petrofabric is considered as random if their spatial distribution is uniform), and (2) twinning is an irreversible process (a characteristic that will be discussed later).

Samples must be accurately oriented in the field. Three perpendicular thin sections are subsequently cut in each sample. This enables one to obtain the most complete spatial coverage of twin orientations, and also to make further geometrical transformations easier.

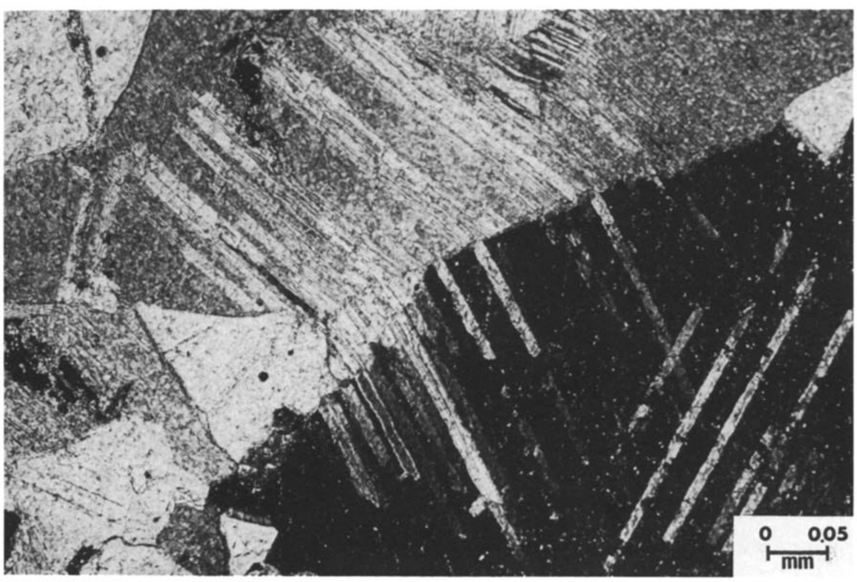


Fig. 5. Thin section (crossed polars) of a limestone collected in Burgundy. Two observable sets of twin lamellae oblique at small angles to the thin section plane, are visible as broad bands which differ from the host by abnormal coloration (compare with Fig. 4).

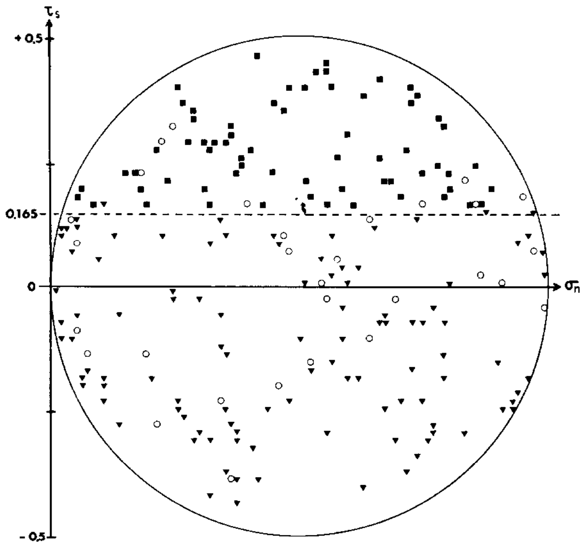


Fig. 6. Example of a normal stress/resolved shear stress diagram for a sample collected at Montagney. $\sigma_n$ = Normal stress; $\tau_s$ = resolved shear stress on each plane. Small black squares represent observed twinned planes which are consistent with the final reduced stress tensor; small black triangles represent observed twinned planes which are inconsistent with the same tensor. Small open circles represent untwinned planes. On this diagram, $\sigma_n$ ranges from 0 to 1, whereas $\tau_s$ ranges from $-0.5$ to $+0.5$ (for theoretical considerations, see Etchecopar, 1984). In the present case, the value of 0.165 is proportional to the twinning threshold (see Tourneret and Laurent, 1990). The dashed line ($\tau_s = 0.165$) separates portions of the diagram where twinned planes are consistent with final solution (above), and where they are not (below). Note that the distribution of twinned planes does not depend on the normal stress $\sigma_n$, in agreement with theory.

The grain size of the studied sample is also an important parameter that must be considered. Several studies have shown that large crystals are twinned more easily than the small ones (Olsson, 1974; Rowe and Rutter, 1990). In the present work, we have only examined sparitic calcite crystals from both cement of oolitic limestones and fossil infills in micritic limestones.

Calcite twin lamellae are examined with a three-axis U-stage, (Figs. 4 and 5). The spatial positions of the *c* axes and poles of *e* twin planes of calcite crystals are then accurately determined (Fig. 7). Finally, the twinned or untwinned character of each potential twin plane is optically checked. Generally, about 30 crystals are examined, for each oriented thin section; this means that for a single sample with three thin sections, about 270 twin planes are taken into account.

The basic assumption is that twinning results from stress related to a single homogeneous average tensor, in such a way that the difference $\sigma_1 - \sigma_3$($\sigma_1$ = maximum principal stress; $\sigma_3$ = minimum stress) is larger than twice the twinning threshold (Laurent et al., 1990). All the *e* planes, twinned and untwinned (Fig. 7), are taken into account in order to compute the tensor solution. As for fault slip data, the working process consists of the inversion of data obtained through microscopic analysis, in order to determine a tensor which accounts for the largest number of twins. For each twin system, this tensor fulfils the requirement that the value of the computed resolved shear stress is equal to (or larger than) the threshold for twinned planes, and simultaneously smaller than the threshold for the untwinned planes. In our study we have adopted the computer technique improved by Etchecopar (1984): the mathematical considerations are exposed in detail in Tourneret and Laurent (1990), and will not be described here. This process yields the directions of the three principal stresses $\sigma_1$, $\sigma_2$ and $\sigma_3$, as well as the value of the ratio $\Phi = (\sigma_2 - \sigma_3)/(\sigma_1 - \sigma_3)$ between principal stress values. The separation of different stress tensors from calcite twin data will be explained in another section of this paper.

*Macroscopic scale: fault slip analysis*

Paleostress reconstruction in fault tectonics is based on the inversion of fault slip data collected in the field (Angelier, 1984, 1989). It consists of determining the average stress state that can be characterized by a stress tensor. This stress tensor corresponds to the orientation of the three principal stresses $\sigma_1$, $\sigma_2$ and $\sigma_3$ and to the ratio $\Phi = (\sigma_2 - \sigma_3)/(\sigma_1 - \sigma_3)$.

The basic assumption is that the orientation of a given fault plane does not necessarily depend on the orientation of the principal stresses. For any inherited discontinuity, only the relative motion of the two blocks on both sides of the fault plane is significant. Moreover, this assumption of slip parallel to shear stress on a given plane is made for both inherited and newly formed faults. This allows one to take into account non-conjugate as well as conjugate shears. In such an analysis, fault interactions and more generally all the variations of average stress axes and of the ratio $\Phi$ inside rock are considered to be negligible. Exceptions need to be controlled by means of careful, qualitative observations.

According to the basic model, slickenside lineations should correspond to the direction and sense of the greatest shear stress (Bott, 1959). If the direction and sense of motion on fault planes are known, computing a particular solution with four unknowns (the reduced stress tensor) is possible. If a tensor $T$ is a solution of the inverse problem, any tensor $kT + lI$ (with $k > 0$) is also a solution (see Angelier, 1989); as a consequence, the final tensor will be an affine function of $T$. In order to compute $T$ and to evaluate the quality of the determination, a function $F$ is defined; $F$ commonly depends on the angle between the actual slip (observed from striations on the fault plane) and the computed shear stress. For the present study, a "direct inversion method" has been adopted with the function $F$ referred to as $S_4$ in Angelier (1984). The optimization process consists of minimizing $F$ according to the least-squares method, so that the minimal value of $F$ corresponds to the best average stress tensor. One finally obtains $T$ and thus the directions of the three principal stress axes $\sigma_1$, $\sigma_2$ and $\sigma_3$, as well as the value of the ratio $\Phi$.

*Separation of different paleostress tensors*

*Using striated microfaults*

Despite the horizontal attitude of the rock formations we studied (showing that the total deformation remains very small), the most striking character of the area of interest is the predominance of polyphase tectonics. In fact, all examined sites displayed superposed structures, so that a

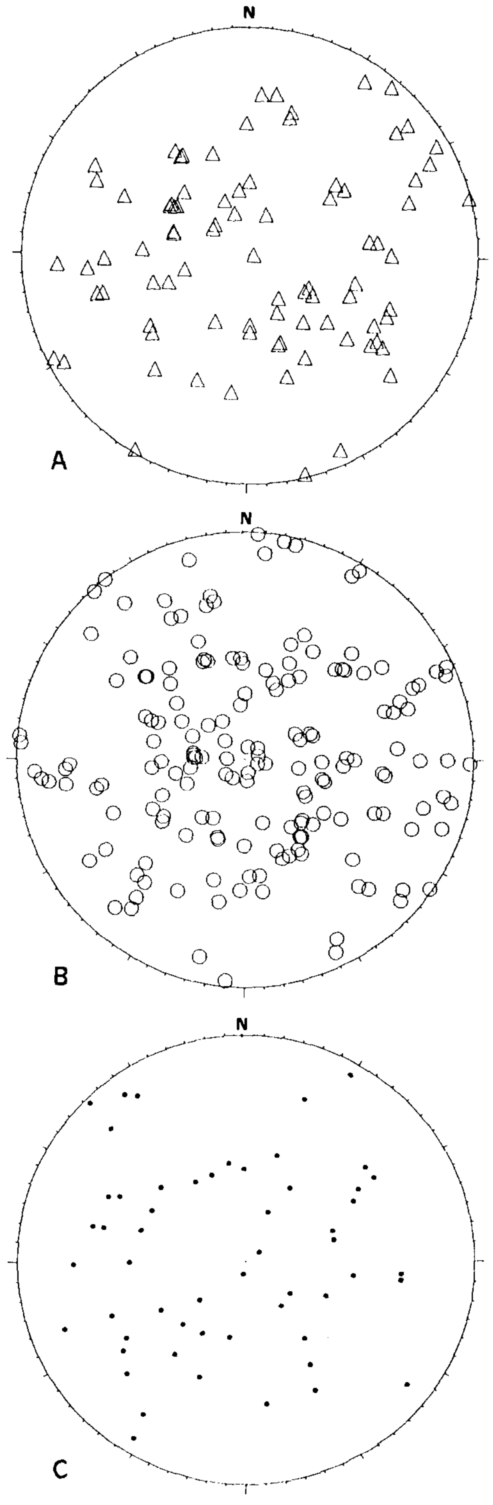


Fig. 7. Stereographic projection of $C$-axes (A, empty triangles) poles of twinned planes (B, empty circles), and poles of untwinned planes (C, black dots) for crystals from the sample collected at Taxenne using Schmidt's equal area projection. The spatial distribution of poles of $e$ planes and of $c$-axes is close to uniform, showing that there is no preferential crystal orientation in the sample.

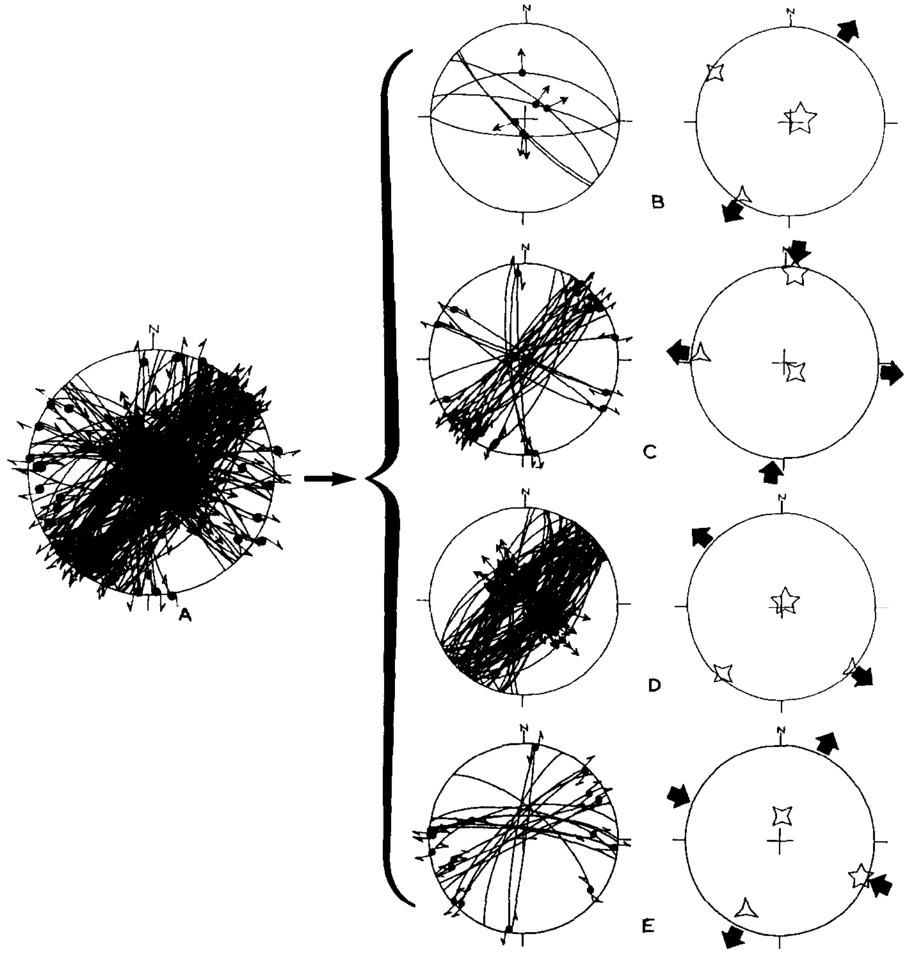


Fig. 8. Example of paleostress analysis with striated faults at Prauthoy locality: separation of subsets of data corresponding to different paleostress states. Fault slip data: diagrams (Schmidt's lower hemisphere projection) with faults as thin curves and slickenside lineations as dots with double arrows (left- or right-lateral) or simple ones (centrifugal-normal; centripetal-reverse). Paleostress directions from fault slip analysis: empty stars with five branchs = maximal compressive stress $\sigma_1$; four branchs = middle stress $\sigma_2$; three branchs = minimal stress $\sigma_3$. Direction of extension or compression shown by large black arrows. A. Entire data set (without any selection). B. Predominantly normal faults consistent with NNE–SSW extension. C. Predominantly strike-slip faults consistent with N–S compression and E–W extension. D. Predominantly normal faults consistent with NW–SE extension. E. Predominantly strike-slip faults consistent with WNW–ESE compression and NNE–SSW extension.

separation of different tectonic events was required (Fig. 8).

*Qualitative separation.* A qualitative separation of successive tectonic events can be carried out according to three main criteria:

(1) The relative chronology of tectonic features is usually based either on the identification of successive movements on a simple structure (such as superposed slickenside lineations of different directions on a fault plane, tension gashes reactivated as normal faults, and so on), or on the intersections of distinct features (e.g., a tension gash cut and offset by a fault).

(2) Normal faults, reverse faults and strike-slip faults are assumed to be systematically distributed in separate subsets, in order to distinguish stress states that correspond to different mechanisms of brittle deformation.

(3) Previous reconstructions of regional tectonic

evolution (Bergerat, 1985, 1987) are taken into account in order to propose a succession of the different tectonic tensors.

*Quantitative separation.* The separation of the different stress tensors and related classes of data is made using an algorithm exposed in Angelier and Manoussis (1980) and Angelier (1984). Where fault data sets are polyphase, the numerical analysis in terms of tensor computation may yield poor results, unless a preliminary qualitative selection (commonly based on the use of relative chronology criteria) is carried out in order to identify the major tectonic events. However, more complex numerical methods may also solve this problem of polyphase fault data by determining simultaneously two or several stress tensors for a given data set (Angelier and Manoussis, 1980; Etchecopar et al., 1981; Angelier, 1984), the classification of each datum depending on the comparison of individual misfits with the tensor.

*Using calcite twins*

As mentioned in an earlier section, the inverse method proposed by Etchecopar (1984) and set out in detail in Tourneret and Laurent (1990) has been adopted in our study. As most of our samples are concerned with polyphase deformation, determination of a single stress tensor compatible with the entire data set (twinned and untwinned planes) is meaningless. For polyphase samples, the process consists of first searching for an initial solution by a random selection of many tensors which are applied to all the data, and then determining the optimal percentage of twinned planes consistent with the request stress tensor. This percentage is first arbitrarily chosen, and then modified to reach the best solution according to a given penalization function (referred to as $F$ in Tourneret and Laurent, 1990). Second, the tensor solution is optimized with regard to the subset of data. When a first tensor is determined, the twinned planes consistent with it are withdrawn, and the process is repeated. We have to bear in mind that even if the existence of untwinned planes is an important constraint for the determination of all stress tensors, it is clear that several twinned planes can be consistent with two or three different tensors. To partially account for this difficulty, a systematic exploration of the solution space is undertaken, using a very large number of random trials. This leads to the determination of the maximum percentage of twins consistent with each stress tensor. Thus, this methodology allows the determination of several stress tensors, but is less accurate than that which could be expected with striated microfaults. Note, finally, that at the present stage of our knowledge, the optical analysis of calcite twins does not provide any evidence of twinning successions, and hence of the relative chronology between the different events. The only way to relate the different episodes of twinning to tectonic events known from geological data still consists of comparing stress tensors obtained from calcite twin analysis with those independently obtained from fault slip analysis.

## Results: paleostress evolution in Burgundy

Four main regional paleostress systems have been defined in the area of Fig. 2. The main characteristics of the tensors computed from fault slip analysis and from calcite twin analysis respectively are shown in Figs. 9–13, and in Tables 1 and 2.

### *NNE–SSW extension*

Tectonic analysis using both methods shows clearly the existence of a NNE–SSW first direction of extension, mostly characterized by normal faults which trend between 85° and 115° (in some cases 60°–115°). The trend of the principal minimal stress, $\sigma_3$, independently computed from faults and calcite twins, is nearly constant at 20°–35° (60° in one case; Fig. 9).

Scarce relative chronology criteria suggest that this extension event occurred prior to a N–S compression, for which we proposed a late Eocene age. But the age of this extension cannot be exactly defined in the area of interest from stratigraphic data because, in all sites studied, rock formations

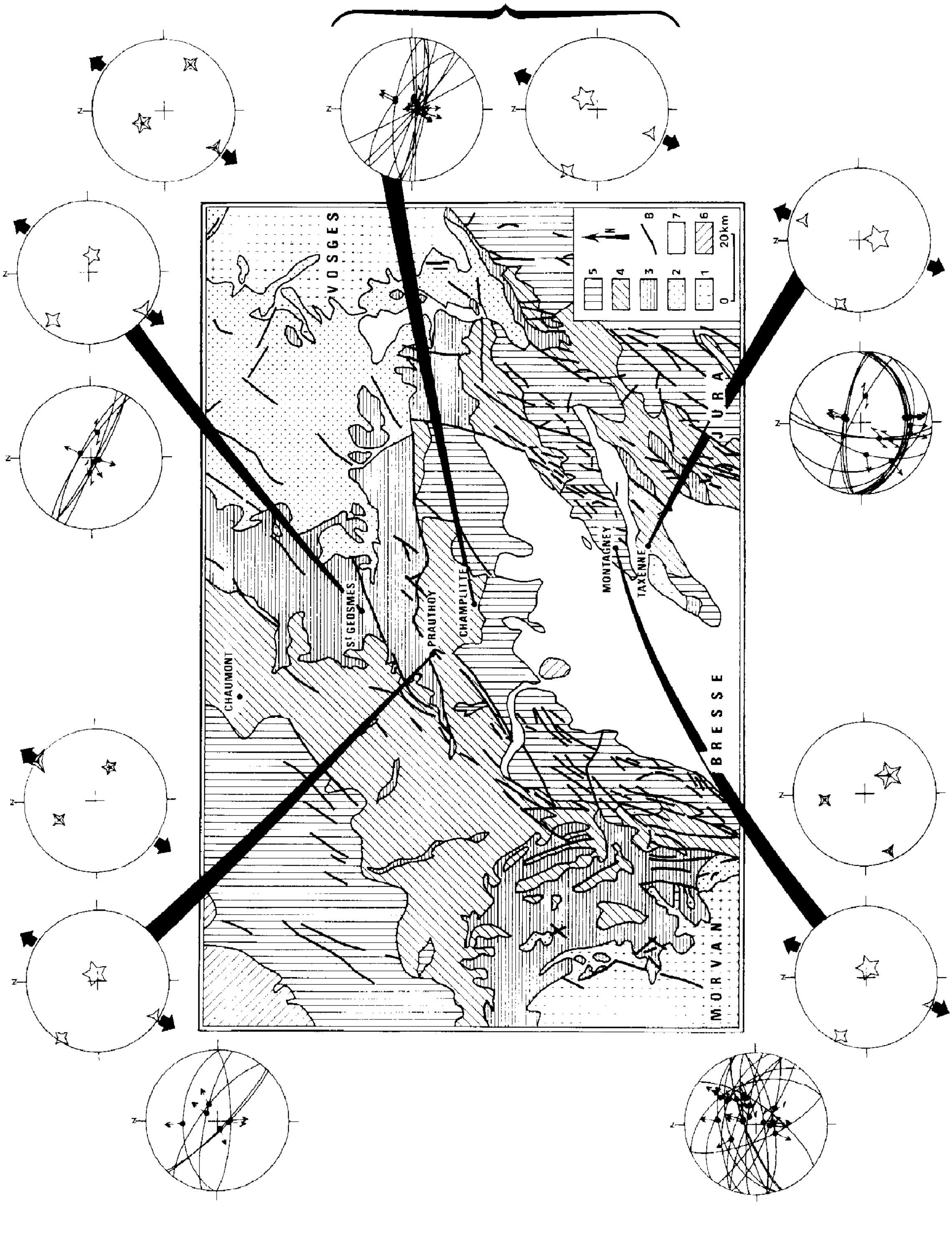


Fig. 9. NNE–SSW extension inferred from microstructural analysis on the northeastern side of the Bresse rift, using fault slips and calcite twins. *Caption (valid for Figs. 9–12)*: Fault slip data: diagrams (Schmidt's lower hemisphere projection) with faults as thin curves and slickenside lineations as dots with double arrows (left-or right-lateral) or simple ones (centrifugal-normal; centripetal-reverse). Stylolitic peaks as black diamonds and tension gashes as empty squares (where present). Paleostress directions from fault slip analysis: empty stars with five branchs = maximal compressive stress $\sigma_1$; four branchs = middle stress $\sigma_2$; three branchs = minimal stress $\sigma_3$. Direction of extension or compression shown by large black arrows. Paleostress directions from calcite twin analysis: ornate stars, with 5, 4 or 3 branchs (as for fault slip analysis). Explanation of *1–9* on geological map, see Fig. 2.

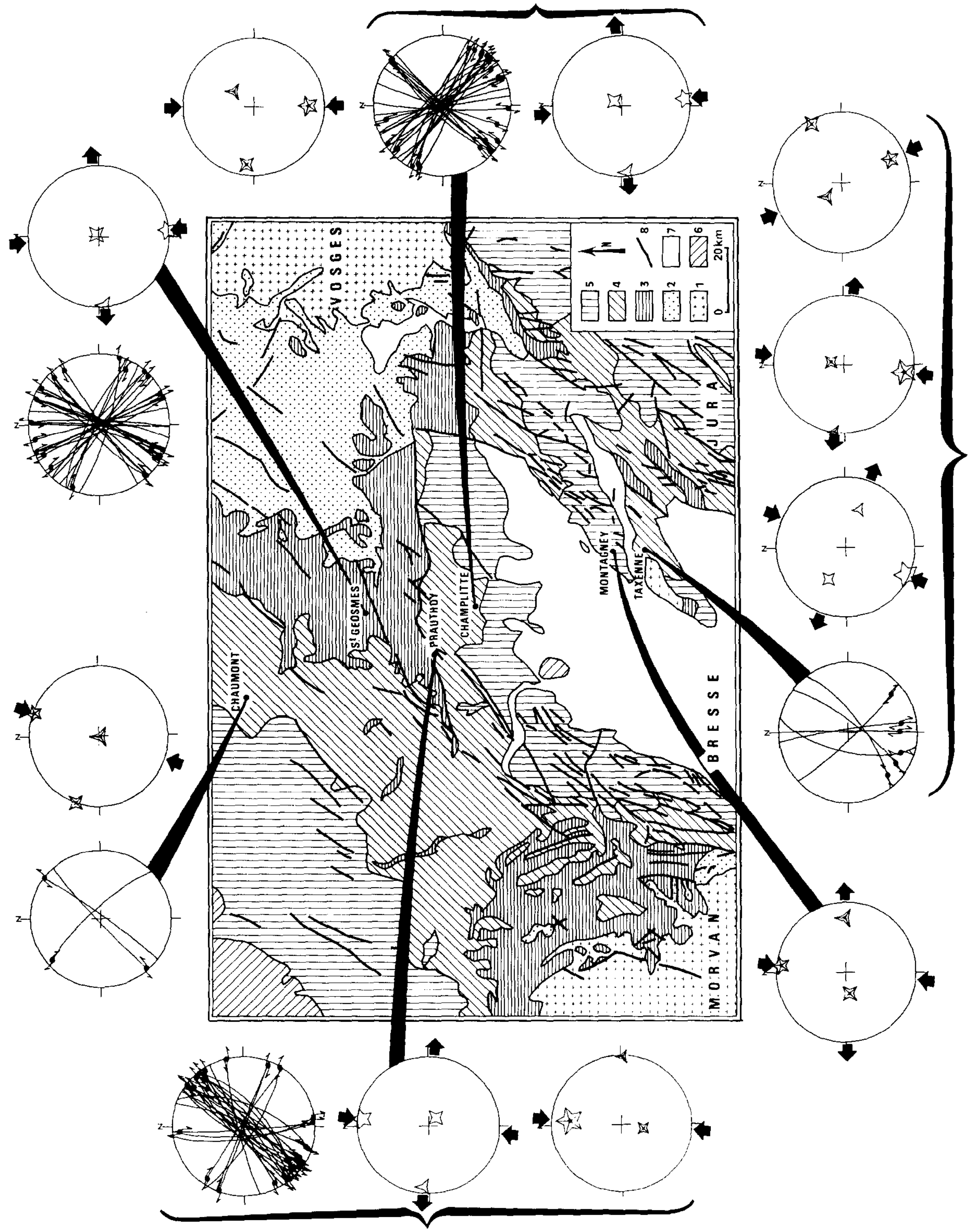


Fig. 10. N–S compression inferred from microstructural analysis on the northeastern side of the Bresse rift, using fault slips and calcite twins. Caption as for Fig. 9.

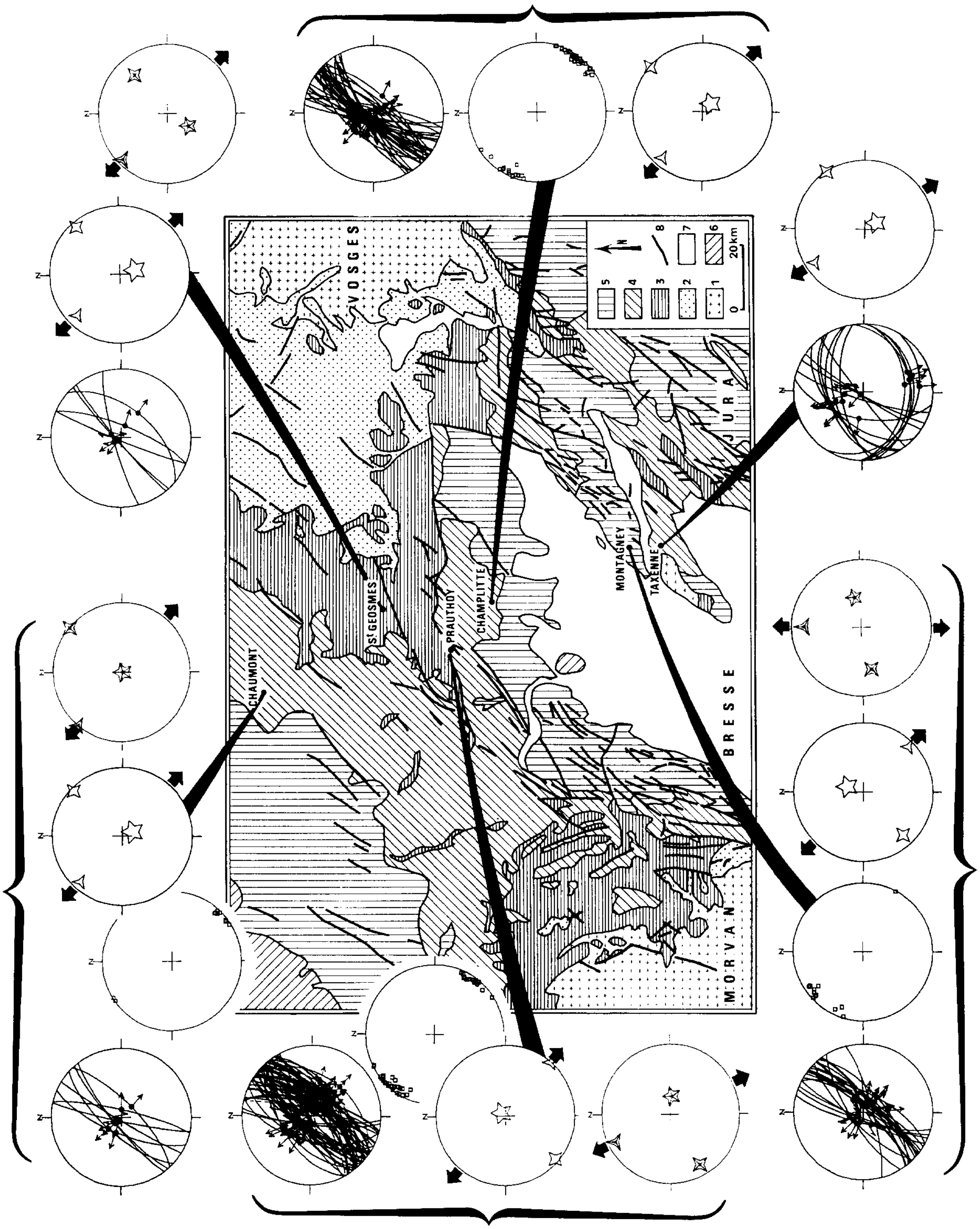


Fig. 11. NW–SE extension inferred from microstructural analysis on the northeastern side of the Bresse rift, using fault slips and calcite twins. Caption as for Fig. 9.

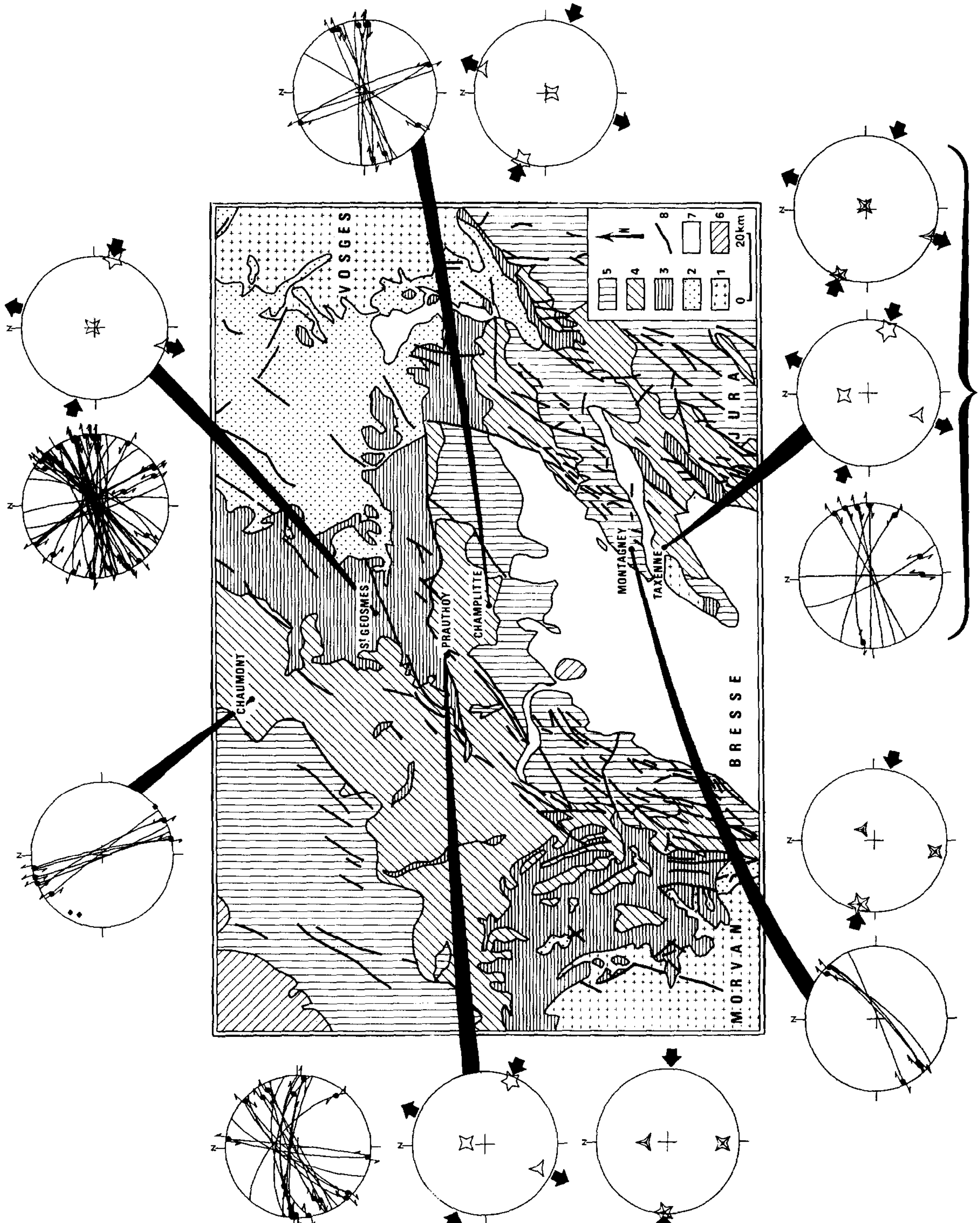


Fig. 12. WNW–ESE compression inferred from microstructural analysis on the northeastern side of the Bresse rift, using fault slips and calcite twins. Caption as for Fig. 9.

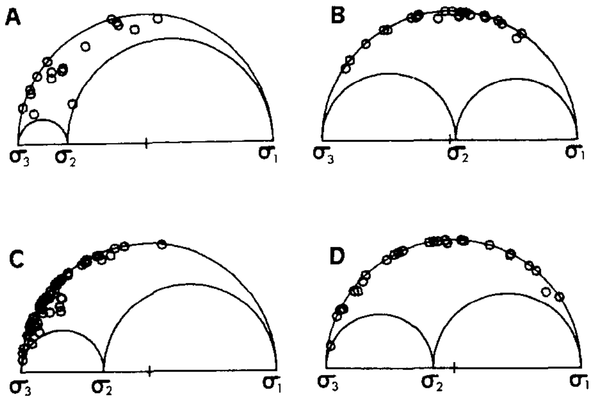


Fig. 13. Examples of dimensionless Mohr diagrams obtained from fault slip data. Abscissae = normal stress; ordinates = shear stress. Position of $\sigma_2$ between $\sigma_3$ and $\sigma_1$, defined according to ratio $\Phi$: $\Phi = (\sigma_2 - \sigma_3)/(\sigma_1 - \sigma_3)$. Each dot corresponds to a fault slip. A. NNE–SSW extension at Montagney; 17 faults, $\Phi = 0.2$. B. N–S compression at Champlitte; 24 faults, $\Phi = 0.5$. C. NW–SE extension at Prauthoy; 74 faults, $\Phi = 0.3$. D. WNW–ESE compression at St Geosmes; 30 faults, $\Phi = 0.4$.

are older than the late Mesozoic and thus predate all the tectonic events under investigation.

The same direction of extension (NNE–SSW) has been already found in the Quercy (Bonijoly and Bles, 1983), in the Limagnes grabens, the northern part of the Alpilles, and the Swabian and the Franconian Juras (Bergerat, 1985) as well as in the Lorraine Basin (Villemin, 1986). According to these authors, the age of this event is probably late Mesozoic. However, Coulon and Frizon de Lamotte (1988) have found evidence in the eastern portion of the Paris basin that a NNE–SSW extension occurred just after the NW–SE extension and prior to the WNW–ESE compression (for which they propose an Oligocene and a Miocene age respectively): they consequently proposed an Oligocene age for the NNE–SSW extension. Our relative chronology criteria, in the area studied, are more in agreement with a late Mesozoic age: the NNE–SSW extension is probably older than the widespread N–S compression, which is unanimously considered as late Eocene in age (see next subsection). However, these results, are compatible because areas under investigation are different and NNE–SSW extension may have occurred twice.

*N–S compression*

A clear regional paleostress system characterized by a N–S horizontal compression have been determined. The main brittle structures related to this tectonic event are conjugate strike-slip faults: left-lateral strike-slip faults show azimuths 20°–60°, whereas right-lateral strike-slip faults range from azimuths 120° to 160°. The trend of $\sigma_1$, computed from fault slip and calcite twin data, is fairly homogeneous for the examined sites; it ranges between 175° and 205° (Fig. 10 and Tables 1 and 2). Subhorizontal and nearly N–S-oriented stylolitic peaks are also consistent with this N–S compression (Fig. 10).

In the studied area, the age of this tectonic event is difficult to establish because Cenozoic formations are absent in convenient outcrops. However, numerous fault planes trending 20°–60° show superposition of two sets of slickensides; in such cases, the first set of striae indicates a strike-slip sense of slip (horizontal or oblique), whereas the second one indicates a normal slip. We conclude that strike-slip faulting has occurred prior to a second event of normal faulting (see next subsection), which can be related to the Oligocene development of the Bressan rift (Rat, 1976; Bergerat, 1987). It is thus reasonable to relate this N–S compressional event to the Pyreneo-Provençal phase, late Eocene in age, following various authors who identified this major tectonic event in different regions of the European platform (De Charpal et al., 1974; Letouzey and Trémolieres, 1980; Mattauer and Mercier, 1980; Arthaud and Seguret, 1981; Bergerat, 1985, 1987).

*NW–SE extension*

This extensional tectonic event induced normal faults associated with numerous tension gashes (Fig. 11). These extensional features are especially abundant close to the Saône graben, which belongs to the Oligocene West European Rift. Near this major graben, both newly formed normal faults and 20° to 60° strike-slip faults reactivated as normal faults can be observed. This event is also clearly characterized at the microscopic scale (Fig. 11, Table 2). Note that both methods indi-

TABLE 1

Main characteristics of paleostress tensors computed from fault slip analysis

| Sites | Stress axes | | Φ | N | Angle (°) |
|---|---|---|---|---|---|
| Taxenne | 177 | 69 | | | |
| | 287 | 08 | 0 | 15 | 6 |
| | 020 | 19 | | | |
| | 205 | 04 | | | |
| | 299 | 47 | 0.1 | 6 | 14 |
| | 111 | 43 | | | |
| | 149 | 75 | | | |
| | 056 | 01 | 0.3 | 16 | 6 |
| | 326 | 15 | | | |
| | 108 | 12 | | | |
| | 355 | 62 | 0.3 | 8 | 12 |
| | 204 | 25 | | | |
| Montagney | 104 | 79 | | | |
| | 294 | 11 | 0.2 | 17 | 14 |
| | 203 | 04 | | | |
| | 018 | 70 | | | |
| | 227 | 17 | 0.3 | 23 | 21 |
| | 134 | 09 | | | |
| Champlitte | 040 | 71 | | | |
| | 296 | 05 | 0.2 | 11 | 15 |
| | 204 | 19 | | | |
| | 174 | 00 | | | |
| | 032 | 80 | 0.5 | 26 | 11 |
| | 265 | 06 | | | |
| | 136 | 76 | | | |
| | 040 | 01 | 0.3 | 39 | 22 |
| | 310 | 13 | | | |
| | 290 | 02 | | | |
| | 182 | 83 | 0.4 | 10 | 9 |
| | 020 | 07 | | | |
| | 062 | 07 | | | |
| | 329 | 22 | 0 | 15 | 16 |
| | 168 | 67 | | | |
| Prauthoy | 072 | 81 | | | |
| | 303 | 05 | 0.2 | 6 | 12 |
| | 212 | 07 | | | |
| | 006 | 03 | | | |
| | 127 | 85 | 0.4 | 30 | 10 |
| | 276 | 05 | | | |

TABLE 1 (continued)

| Sites | Stress axes | | Φ | N | Angle (°) |
|---|---|---|---|---|---|
| Prauthoy | 035 | 85 | | | |
| | 221 | 06 | 0.3 | 74 | 15 |
| | 131 | 01 | | | |
| | 113 | 07 | | | |
| | 005 | 69 | 0.5 | 17 | 14 |
| | 206 | 20 | | | |
| St Geosmes | 103 | 70 | | | |
| | 307 | 18 | 0.6 | 5 | 16 |
| | 215 | 08 | | | |
| | 175 | 02 | | | |
| | 045 | 86 | 0.5 | 25 | 7 |
| | 265 | 03 | | | |
| | 166 | 72 | | | |
| | 049 | 09 | 0.2 | 6 | 21 |
| | 316 | 16 | | | |
| | 105 | 00 | | | |
| | 014 | 87 | 0.4 | 30 | 11 |
| | 195 | 02 | | | |
| Chaumont | 157 | 77 | | | |
| | 043 | 05 | 0.2 | 8 | 17 |
| | 312 | 12 | | | |

Stress axes: trend and plunge of each stress axis, in degrees. Φ $(\sigma_2-\sigma_3)/(\sigma_1-\sigma_3)$, defined in text. $N$ = number of fault slip data; Angle = average angle computed shear stress—observed slickenside lineation, in degrees

cate a NW–SE direction of extension, whereas the trend of Oligocene extension is more generally E–W along the West European Rift in the European platform (Bergerat, 1985, 1987). Note also that in the area of interest, the E–W extension is absent. We propose to consider that this NW–SE direction of extension is due to regional stress perturbations near the transition zone between the Rhinegraben and the Saône graben (Lacombe et al., 1990). This tectonic event is thus related to the major extensional phase of the West European rifting that occurred during the Oligocene (Bergerat, 1987).

*WNW–ESE compression*

According to relative chronology data, a WNW–ESE compression is the last tectonic event

TABLE 2

Main characteristics of paleostress tensors computed from calcite twin analysis

| Sites | Stress axes | | Φ | $N_1$ | $N_2$ | $N_3$ |
|---|---|---|---|---|---|---|
| Taxenne | 188 | 15 | | | | |
| | 012 | 75 | 0.1 | 172 | 51 | 29 |
| | 278 | 01 | | | | |
| | 293 | 03 | | | | |
| | 064 | 86 | 0.6 | 143 | 51 | 42 |
| | 203 | 03 | | | | |
| | 156 | 23 | | | | |
| | 063 | 07 | 0.5 | 101 | 51 | 20 |
| | 317 | 66 | | | | |
| Montagney | 006 | 07 | | | | |
| | 260 | 65 | 0.6 | 183 | 31 | 73 |
| | 089 | 24 | | | | |
| | 078 | 53 | | | | |
| | 258 | 37 | 0.6 | 110 | 31 | 44 |
| | 002 | 19 | | | | |
| | 283 | 09 | | | | |
| | 191 | 16 | 0.3 | 69 | 31 | 27 |
| | 044 | 72 | | | | |
| | 144 | 55 | | | | |
| | 352 | 43 | 0.04 | 42 | 31 | 16 |
| | 247 | 14 | | | | |
| Prauthoy | 005 | 27 | | | | |
| | 190 | 64 | 0.02 | 190 | 41 | 119 |
| | 092 | 02 | | | | |
| | 273 | 02 | | | | |
| | 182 | 24 | 0.5 | 102 | 41 | 30 |
| | 359 | 65 | | | | |
| | 114 | 48 | | | | |
| | 333 | 42 | 0.9 | 102 | 41 | 25 |
| | 035 | 02 | | | | |
| St Geosmes | 179 | 24 | | | | |
| | 277 | 16 | 0.4 | 134 | 59 | 49 |
| | 038 | 61 | | | | |
| | 330 | 61 | | | | |
| | 120 | 26 | 0.4 | 89 | 59 | 35 |
| | 216 | 12 | | | | |
| | 211 | 61 | | | | |
| | 049 | 28 | 0.5 | 67 | 59 | 26 |
| | 315 | 08 | | | | |
| Chaumont | 020 | 02 | | | | |
| | 290 | 00 | 0.7 | 115 | 16 | 34 |
| | 198 | | 88 | | | |

TABLE 2 (continued)

| Sites | Stress axes | | Φ | $N_1$ | $N_2$ | $N_3$ |
|---|---|---|---|---|---|---|
| Chaumont | 199 | 89 | | | | |
| | 040 | 01 | 0.4 | 115 | 16 | 51 |
| | 310 | 00 | | | | |

Same caption for stress axes and Φ value as in Table 1. $N_1$ = Number of measured twinned planes; $N_2$ = number of measured untwinned planes; $N_3$ = number of twinned planes compatible with the solution

that we could definitely recognize in the field. The trend of the $\sigma_1$ axis provided by the two methods is nearly constant, ranging from 273° (from calcite twins) to 113° (from fault slips) (Fig. 12 and Tables 1 and 2). The compression is characterized in some cases by reactivation of several earlier strike-slip faults (30°–60°, 140°–160°, consistent with the N–S compression), and in others by numerous newly formed faults with azimuths ranging from 115° to 190°. This provides evidence that this event occurred after the N–S compression. The exact age of this event is difficult to establish, and will not be discussed here. Nevertheless, these brittle structures are probably contemporaneous with the Pontian westward thrusting of Jura (Caire, 1974; Bergerat, 1985).

*Enigmatic NE–SW compression*

In one site (Champlitte), our field study demonstrates the existence of a NE–SW compression (Table 1). This paleostress regime caused left-lateral strike-slip faults ranging from 70° to 90° in strike, and right-lateral motion of inherited N–S to NNE–SSW trending faults.

According to Bergerat (1985, 1987), a compressional event of this direction is related to an early Miocene deformation of the European platform. But we could only reliably determine one tensor corresponding to this orientation (Table 1). In the sites of St. Geosmes and Chaumont, some strike-slip faults are consistent with the same direction of compression, but data are scarce. Moreover, calcite twin analysis did not provide reliable tensors that could be related to this deformation phase. This NE–SW compression will not be dis-

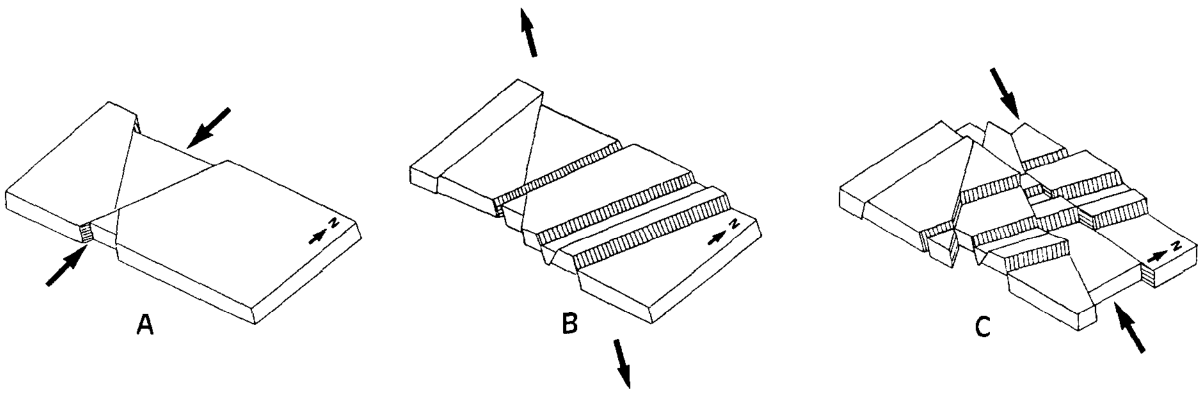


Fig. 14. Schematic diagrams of Cenozoic polyphase tectonics of Burgundy. A. N–S compression, principally inducing conjugate strike-slip faults that strike N–S and NE–SW (left-lateral) and NW–SE (right-lateral). Event related to "Pyreneo-Provencal" phase, late Eocene in age (Mattauer and Mercier, 1980; Arthaud and Seguret, 1981; Bergerat, 1987). B. NW–SE extension, principally reactivating left-lateral strike-slip faults of the previous compressional event as normal faults trending nearly 030°, and creating newly formed normal faults. Event related to the West European rifting, Oligocene in age (Bergerat, 1987). C. WNW–ESE compression, principally reactivating right-lateral strike-slip faults of the first compressional event as left-lateral strike-slip faults, and creating new right-lateral strike-slip faults. Event related to the "Pontian" phase of Jura thrusting (Alpine compression: Caire, 1974; Bergerat, 1987).

cussed hereafter, because this event could not be identified with certainty in the area studied.

## Discussion

### *Regional and geodynamical aspects*

All the events defined above affected the Burgundy platform during Mesozoic and Cenozoic times. Our reconstruction is in good agreement with previous descriptions of polyphase tectonics and structural evolution in this area (Fig. 14), as discussed by Bergerat (1977, 1985, 1987) and Gélard (1978). The directions of paleostresses determined from both fault slip and calcite twin analyses can be mapped, as Fig. 15 shows. Although our sites are not sufficiently numerous, a clear picture of average paleostress orientations emerges from this figure.

The tectonic phases characterized in our study can be correlated with the successive paleostresses exerted on the boundaries of the Eurasiatic plate during the different stages of Africa–Eurasia collision (Le Pichon et al., 1988), as follows.

(1) The whole of the European platform recorded, during the late Eocene, a horizontal maximum principal stress $\sigma_1$ trending N–S (Fig. 10). This widespread N–S compression (Mattauer and Mercier, 1980) can be interpreted as a consequence of the collision of the Iberian peninsula with Eurasia, following its motion towards the NNW (Bergerat, 1987).

(2) During the Oligocene, differential motion occurred between the main part of Eurasia and western Europe (Savostin et al., 1986): it resulted in a major change of the stress field from compressional to extensional, and intraplate crustal stretching between western and central Europe. A major line of weakness, the future West European Rift, thus developed with a E–W to NW–SE direction of extension (Fig. 11).

(3) The WNW–ESE direction of compression recorded inside the Alpine and the Jurassian foreland (Fig. 12) is easily correlated with the NW–SE convergence of Africa and Eurasia and the associated Miocene collision.

In conclusion, in the studied area, as well as in other regions of the European platform, the Cenozoic recorded paleostresses (N–S compression, E–W to NW–SE extension, WNW–ESE compression) fit a simple paleostress model: this model takes into account the shape of major plate boundaries and the known relative velocity vectors across these boundaries, especially across the Africa–Eurasia plate boundary (Bergerat, 1985; Letouzey, 1986; Le Pichon et al., 1988); the NNE–SSW extension, probably late Mesozoic in age as discussed above, could not be correlated to any accurate kinematic information available at the present time; however, this extensional event is consistent with the Mesozoic evolution of the Tethys belt (Dercourt et al., 1986).

*Methodology: comparison of the two methods*

*Consistency of results obtained with the two methods*

The most important point which comes from this study is the demonstration of the internal consistency of results obtained by calcite twin analysis at the regional scale. As already shown, all paleostress directions that have been characterized with this method at each data collection site are quite similar to those obtained at the other sites. Moreover, the corresponding tensors can be accurately correlated with tensors computed independently from fault slip analysis, as Fig. 15 shows. We conclude that the calcite twin method fits the following major requirements:

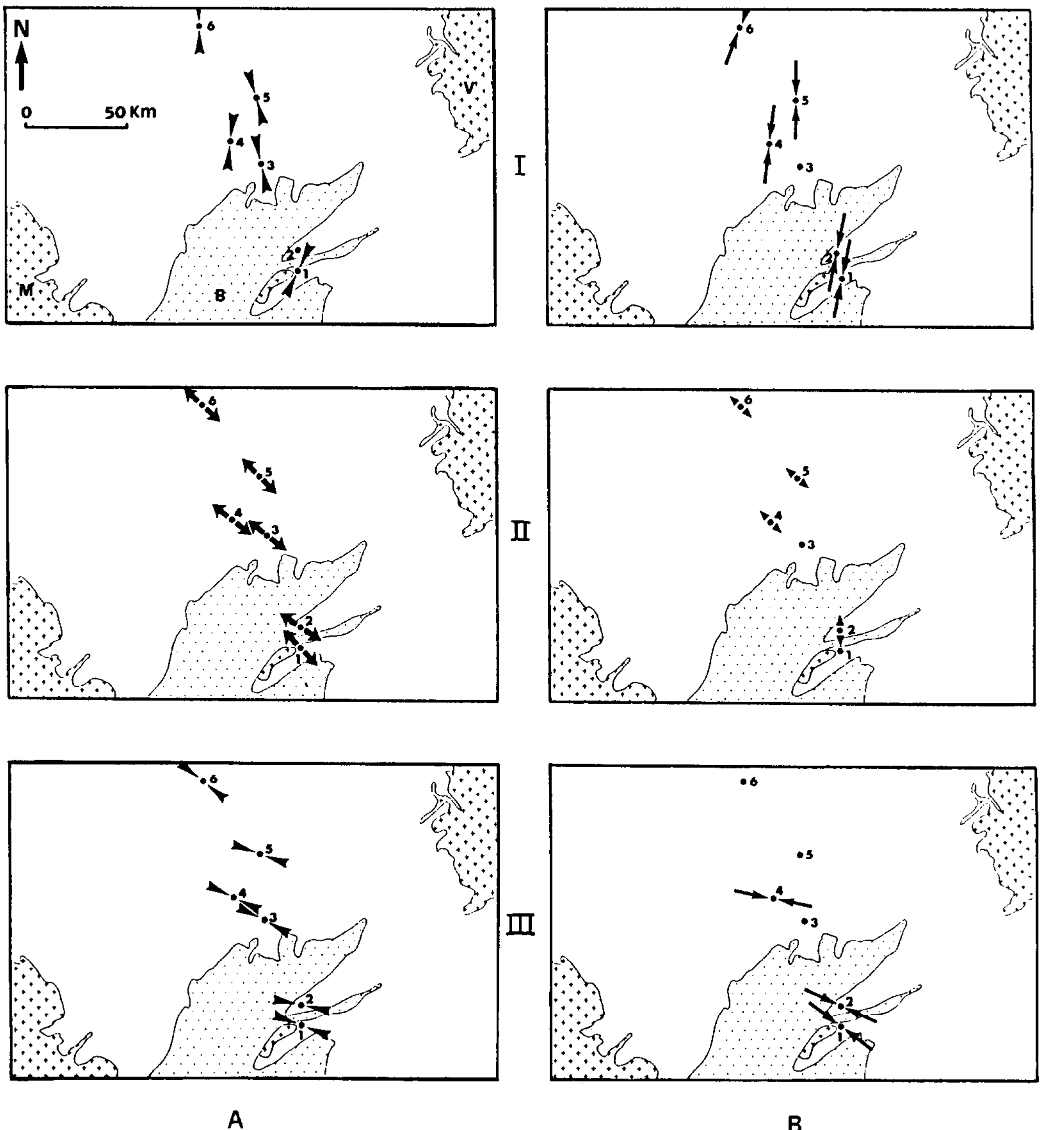


Fig. 15. Paleostress directions reconstructed from fault slip analysis (column A) and calcite twin analysis (column B) for the successive tectonic events which have affected the Burgundy platform during the Cenozoic. Line I = Eocene compression; line II = Oligocene extension; line III = Miocene compression. *1–6* = Sites of data collection: *1* = Taxenne; *2* = Montagney; *3* = Champlitte; *4* = Prauthoy; *5* = St Geosmes; *6* = Chaumont. *V* = Vosges; *B* = Bressan rift; *M* = Morvan; Hercynian basement shown as a pattern of crosses; Tertiary graben shown as a dotted pattern.

(1) It provides consistent results through application at a regional scale.

(2) It allows the computation of several paleostress tensors which can be related to different tectonic events, in a clearly defined polyphase tectonics setting.

(3) It provides paleostress tensors that can easily be related to those obtained independently from fault slip data and to regional geological data.

At several sites, some paleostress tensors could not be computed with one of the two methods; for example, outcrops of the Montagney site contain few measurable strike-slip faults consistent with the N–S compression. As a consequence, computing the corresponding paleostress tensor was not possible, but a well-defined tensor with a $\sigma_1$ axis trending near the azimuth 6° (see Fig. 10) has been obtained from calcite twin analysis. In contrast, for the WNW–ESE compression at St. Geosmes or for the NW–SE extension at Taxenne, tensors could be obtained only from fault slip analysis. Thus, for a given outcrop of limestones, and for a given tectonic event, rupture can occur without twinning, whereas in the same outcrop and for a second tectonic event, both deformations occur simultaneously. That means that in this case, the variation of the size of calcite grains has little influence on the occurrence of mechanical twinning. According to Etchecopar (1984) or Larroque and Laurent (1988), rupture and twinning occur simultaneously only inside a restricted domain of confining pressure. Consequently, for a given value of confining pressure, one of these two types of deformation (twinning and rupture) may occur while the other does not. This provides further evidence that both methods are complementary, and should be used jointly for extensive accurate paleostress analyses at the regional scale. Generally, one cannot determine in advance precisely what the conditions of deformation were at a given site at the time of the successive tectonic events, and then which of the two methods is most appropriate.

At the site of Taxenne (the southernmost site of the profile; see location on Fig. 2), two different paleostress tensors computed from calcite twins with horizontal and vertical $\sigma_3$ axes respectively, correspond to N–S $\sigma_1$ axes and thus can be related to the N–S compression (Fig. 10). This indicates that a strike-slip paleostress state with horizontal $\sigma_3$ (I) *and* a compressive paleostress state with vertical $\sigma_3$ (II) can develop with almost the same horizontal $\sigma_1$ axis. In other words, two different paleostress states may occur during the same major tectonic event; in detail, there is an additional rotation of the $\sigma_1$ axis (from azimuth 188° to 156°). Although further studies are needed, we suppose that type II has occurred second, as a possible consequence of a reduction of lithostatic overburden. Such stress changes within a single major event have been observed very frequently in several regions from fault striation analysis (Angelier and Bergerat, 1983; Etchecopar and Mattauer, 1988).

At the other sites, tensors related to the N–S compression have a $\sigma_3$ axis which is either horizontal (Montagney, Prauthoy) or vertical (St. Geosmes, Chaumont). In these last two cases, tensors obtained with both methods are quite consistent for the $\sigma_1$ axis, but they show an inversion between axes $\sigma_2$ and $\sigma_3$ (Fig. 10); this phenomenon could be easily explained with a ratio $\Phi$ close to 0 (case of paleostress inversion of $\sigma_2$ and $\sigma_3$ during a compresional tectonic event with $\sigma_2$ close to $\sigma_3$). However, the ratios $\Phi$ computed using both methods (faults and calcite twins) are close to 0.5. Although no definite explanation has been found, we observe that a strike-slip paleostress state (with horizontal $\sigma_3$) that is well-defined at the macroscopic scale (faults) can be expressed at the microscopic scale (calcite twins) as a pure compressional regime (with vertical $\sigma_3$), with a common axis of principal stress $\sigma_1$; this phenomenon resembles that described in the previous paragraph (Taxenne) for tectonic twinning alone. It probably reflects relatively minor changes during a single major tectonic event.

*Additional contribution of calcite twin analysis*

As discussed in an earlier section, the use of both methods is recommended because of their complementarity. We have shown, however, that these methods provide regionally consistent results so that one can consider that the results obtained at sites where paleostress tensors could be computed with a single method only are reliable. As a consequence, the complementary use of both methods obviously allows more accurate mapping of stress trajectories, especially in weakly deformed areas where microfaults are not sufficiently numerous to determine paleostress tensors: such a study should incorporate sites where both methods are applicable (test of consistency) and sites where a single method is applicable (complementarity).

Paleostress analysis based on fault slip data provides only four of the six parameters of the real stress tensor (see discussion in earlier section): these four parameters describe the orientations of the $\sigma_1$, $\sigma_2$ and $\sigma_3$ axes as well as the ratio $\Phi$ (i.e. one relationship between the magnitudes of $\sigma_1$, $\sigma_2$ and $\sigma_3$). Determination of the missing parameters requires the simultaneous use of additional rupture and friction laws (Angelier, 1989). Because the twinning threshold provided by experiments on calcitic rocks can be considered to be a constant, calcite twin analysis yields magnitudes of differential stresses $\sigma_i - \sigma_j$ (Laurent, 1984; Tourneret and Laurent, 1990). The "calcite method" consequently provides one more parameter than the "fault method": two relationships between the magnitudes of $\sigma_1$, $\sigma_2$ and $\sigma_3$, instead of a single one. Thus, the additional knowledge of the isotropic stress factor is enough to determine the complete stress tensor.

Applied to samples collected in Burgundy, the "calcite method" thus enabled us to assign some limits to the stress magnitudes for the different tectonic events: the corresponding values are listed in Table 3. Note that there is no significant difference between values collected in the southern or in the northern portions of the profile, or between values for the different major phases.

Such an attempt to estimate the magnitudes of stresses producing brittle deformation, especially in the European platform setting, has already been proposed by Bergerat et al. (1982) from experiments upon carbonate rocks sampled in Germany. The values obtained by these experiments are larger than these deduced from calcite twins, and were also considered to be overestimated according to further stress magnitude analyses (Angelier, 1989). The order of magnitude of the stresses

TABLE 3

Values of differential stresses obtained from calcite twin analysis

| Sites | NNE –SSW extension (MPa) | N–S compression (MPa) | NW –SE extension (MPa) | WNW –ESE compression (MPa) |
|---|---|---|---|---|
| Taxenne | – | 32–39 | – | 43 |
| | | 3–21 | | 26 |
| Montagney | 32 | 60 | 55 | 39 |
| | 1 | 35 | 31 | 11 |
| Prauthoy | 33 | – | – | 42 |
| | 29 | | | 20 |
| St Geosmes | 51 | 59 | 40 | 46 |
| | 22 | 25 | 20 | 22 |
| Chaumont | – | 53 | – | – |
| | | 36 | | |

For each site and each tectonic event, the first number indicates the value of $\sigma_1 - \sigma_3$; the second number indicates the value of $\sigma_2 - \sigma_3$ (theoretical considerations not discussed in this paper; see Etchecopar, 1984)

provided by calcite twin analysis (Table 3) is the same as for *in situ* stress determination in central Europe (Greiner and Illies, 1977).

The "fault method" obviously requires large outcrops where sufficiently numerous striated microfaults can be measured. In contrast, calcite twin analysis allows determination of stress tensors from a very restricted rock volume. The possibility of studying very small outcrops where macroscopic fault analyses cannot be carried out due to the lack of data will enable one to increase the accuracy of paleostress trajectory mapping, and consequently to discuss second order regional patterns such as stress perturbations.

*Limits of the calcite twin analysis method*

Twinning is considered as an irreversible process, especially for sharply defined straight twins (Laurent, 1984). This, however, has not been unquestionably demonstrated, and different authors disagree. Figure 6 shows several *twinned* planes, located in the lowest part of the diagram, for which the resolved shear stress has a negative value (close to $-0.5$). That means that, with regard to the orientation of the principal stress axes, the spatial orientation of these twinned planes is such that the corresponding resolved shear stress is quite opposed to the sense of twinning: if twinning was reversible, such twins should have been erased. This observation provides an argument in favour of considering calcite twinning as irreversible to a first approximation. As a consequence, the analysis of calcite twins is convenient for studying polyphase tectonics (this would not be the case if twins could systematically be erased by further events).

In comparison with the "fault method", the existence of polyphase tectonics in some cases imposes a limit on the use of the "calcite method". First, as discussed in an earlier section, calcite twin analysis does not theoretically allow determination of stress tensors as precisely as fault slip analysis. Second, all twins that theoretically develop during two different tectonic events with one common principal stress axis ($\sigma_3$ or $\sigma_1$) are equated to the group of twins which would be obtained from a single phase with a $\Phi$ ratio close to 1 (i.e. $\sigma_2$ close to $\sigma_1$) or 0 (i.e. $\sigma_3$ close to $\sigma_2$). This explains the difficulty of distinguishing several stress regimes with one common principal stress axis ($\sigma_1$ or $\sigma_3$). However, in practice, analyses and computations which have been carried out in this study resulted in very good stress tensors, quite similar to those independently reconstructed by means of fault striation analysis. Thus, although results have to be systematically discussed according to the value of the $\Phi$ ratio, one can consider polyphase tectonics deduced from calcite twin study as reliable. One then has to bear in mind that even if offset of a twin set by a second one can be observed with an electron microscope (Barber and Wenk, 1976), so that relative chronology can be determined, the optical analysis with a U-stage does not, at the present time, provide any evidence of relative chronology between successive tectonic events. Relative chronology can only be determined through comparison with the study of macroscopic features.

*Future prospects*

Up to now, only sparitic calcite crystals which constitute the matrix of examined samples had been analysed (Tourneret, 1987). For the first time, large calcite crystals of fossil infills in micritic limestones have been studied, showing that determination of paleostress orientations in such coarse crystalline infills are reliable. The good quality of our obtained tensors shows that such a new approach is full of promise, and can enlarge the application field of the "calcite method". Finally, as calcite twin analysis enables one to reconstruct paleostresses even where faults are very scarce or are missing and from a very restricted rock volume, it will be very useful for fracture-paleostress analyses on core samples from drill holes.

## Conclusion

The present work is the first attempt to reconstruct paleostresses at a regional scale (see Figs. 2 and 15) using calcite twin analysis: concurrently, an accurate study of macroscopic tectonic features has been carried out in order to allow comparison between this method and that utilizing slickensided faults. Results obtained are consistent along the studied profile; in particular, fault slip analysis and calcite twin analysis provide quite similar paleostress tensors. As a result, the systematically combined use of both methods has enabled us to characterize the main stages of the tectonic evolution of the Burgundy platform since the Late Mesozoic.

The multi-technical approach which has been applied in this study, and which relies upon tectonic analyses, processing and crystallography, provides a very convenient and reliable way to reconstruct paleostresses in platform tectonic setting.

## Acknowledgements

Fieldwork is supported by the GS Tethys and the IFP. Comments by Jan Tullis and an anonymous referee allowed us to make major improvements to the paper.

## References

Angelier, J., 1984. Tectonic analysis of fault slip data sets. J. Geophys. Res., 89, B7: 5835–5848.

Angelier, J., 1989. From orientation to magnitudes in paleostress determinations using fault slip data. J. Struct. Geol., 11: 37–50.

Angelier, J. and Bergerat, F., 1983. Systèmes de contraintes et extension intracontinentale. Bull. Cent. Rech. Explor. Prod. Elf Aquitaine, 7 (1): 137–147.

Angelier, J. and Goguel, J., 1979. Sur une méthode simple de détermination des axes principaux des contraintes pour une population de failles. C.R. Acad. Sci., Paris, 288: 307–310.

Angelier, J. and Manoussis, S., 1980. Classification automatique et distinction des phases superposées en tectonique de failles. C.R. Acad. Sci., Paris, II, 290: 651–654.

Armijo, R. and Cisternas, A., 1978. Un problème inverse en microtectonique cassante. C.R. Acad. Sci., Paris, 287: 595–598.

Arthaud, F. and Seguret, M., 1981. Les structures pyrénéennes du Languedoc et du Golfe du Lion (Sud de la France). Bull. Soc. Géol. Fr., 7, 23, (1): 51–63.

Barber, D.J. and Wenk, H.R., 1976. Defects in deformed calcite and carbonate rocks. In: H.R. Wenk (Coordinating Editor), Electron Microscopy in Mineralogy. Springer, Berlin.

Bergerat, F., 1977. La fracturation de l'avant-pays jurassien entre les fossés de la Saône et du Rhin. Analyse et essai d'interprétation dynamique. Rev. Géog. Phys. Géol. Dyn., (2), XIX (4): 325–338.

Bergerat, F., 1985. Déformations cassantes et champs de contrainte tertiaires de la plate-forme carbonatée européenne. Thèse de Doctorat-es-Sciences, Mém. Sci. Terre, Univ. P. et M. Curie, no. 85-07, Paris, 315 pp.

Bergerat, F., 1987. Stress fields in the European platform at the time of Africa–Eurasia collision. Tectonics, 6: 99–132.

Bergerat, F., Bergues, J. and Geyssant, J., 1982. Estimation des contraintes liées à la formation de décrochements dans la plate forme carbonatée de l'Allemagne du Sud. C.R. Acad. Sci., Paris, 295, II: 1155–1160.

Bonijoly, D. and Bles, J.L., 1983. Histoire tectonique du Quercy (bordure NE du bassin d'Aquitaine. France). Géométrie, cinématique et chronologie des déformations cassantes. Bull. Soc. Géol. Fr., (7), XXV: 775–783.

Bott, M.H.P., 1959. The mechanism of oblique slip faulting. Geol. Mag., 96 (2): 109–117.

Cahn, R.W., 1964. Survey of recent progress in the field of deformation twinning. In: Conference on Deformation Twinning. R.E. Reed-Hill,J.P. Hirth and H.C. Rogers (Editors), Gordon and Breach, New York, pp. 1–28.

Caire, A., 1974. Caractères et conditions du recouvrement tectonique pontien dans la partie occidentale du faisceau salinois (Jura). Les décrochements jurassiens dans le cadre alpin. Actes du 99e Congr. Soc. Sav., Besançon, Sciences, 1: 73–84.

Carey, E. and Brunier, B., 1974. Analyse théorique et numérique d'un modèle mécanique élémentaire appliqué à l'étude d'une population de failles. C.R. Acad. Sci., Paris, (D), 279: 891–894.

Coulon, M. and Frizon de Lamotte, D., 1988. Les extensions cénozoiques dans l'Est du bassin de Paris: mise en évidence et interprétation. C.R. Acad. Sci., Paris, 307, II: 1113–1119.

De Charpal, O., Tremolieres, P., Jean, F. and Masse, P., 1974. Un exemple de tectonique de plate-forme: les Causses majeures (Sud du Massif central, France). Revue I.F.P., 29(5): 641–659.

Dercourt, J., Zonenshain, L.P., Ricou, L.E., Kazmin, V.G., Le Pichon, X., Knipper, C., Grandjacquet, C., Sborshikov, J., Geyssant, J., Lepvrier, C. and Pechersky, D.H., 1986. The geological evolution of the Tethys belt from the Atlantic to the Pamirs since the Liassic. Tectonophysics, 123: 241–315.

Etchecopar, A., 1984. Etude des états de contraintes en tectonique cassante et simulation de déformations plastiques (approche mathématique). Thèse de Doctorat-es-Sciences, Univ. Sciences et Techniques du Languedoc, Montpellier, 270 pp.

Etchecopar, A. and Mattauer, M., 1988. Méthodes dynamiques d'analyse des populations de failles. Bull. Soc. Géol. Fr., 8: 289–302.

Etchecopar, A., Vasseur, G. and Daignieres, M., 1981. An inverse problem in microtectonics for the determination of stress tensor from fault striation analysis. J. Struct. Geol. 3: 51–65.

Friedman, M., 1964. Petrofabric techniques for the determination of principal stress directions in rocks. In: W.R. Judd (Editor), State of Stress in the Earth's Crust. Elsevier, New York, pp. 450–552.

Gelard, J.P., 1978. La fracturation de la Bourgogne méridionale. Essai d'interprétation et implications tectonique régionales. Rev. Géogr. Phys. Géol. Dyn., XX (4): 5–28.

Greiner, G. and Illies, J.H., 1977. Central Europe: active or residual tectonic stresses. Pure Appl. Geophys., 115: 11–26.

Handin, J.W. and Griggs, D., 1951. Deformation of Yule marble. Part II. Predicted fabric changes. Geol. Soc. Am. Bull., 62: 863–886.

Lacombe, O., Angelier, J., Bergerat, F. and Laurent, Ph., 1990. Tectoniques superposées et perturbations de contrainte dans la zone transformante Rhine–Saône: apport de l'analyse des failles et des macles de la calcite. Bull. Soc. Géol. Fr., 5 in press.

Larroque, J.M. and Laurent, Ph., 1988. Evolution of the stress field pattern in the south of the Rhine graben from the Eocene to the present. Tectonophysics, 148: 41–58.

Laurent, Ph., 1984. Les macles de la calcite en tectonique: nouvelles méthodes dynamiques et premières applications. Thèse de Doctorat-es-Sciences, Univ. Sciences et Techniques du Languedoc, Montpellier, 324 pp.

Laurent, Ph., Bernard, Ph., Vasseur, G. and Etchecopar, A., 1981. Stress tensor determination from the study of e twins in calcite: a linear programming method. Tectonophysics, 78: 651–660.

Laurent, Ph., Tourneret, Ch. and Laborde, O., 1990. Determining deviatoric stress tensors from twin lamellae in calcite. Application to monophased synthetic and natural polycrystals. Tectonics, in press.

Le Pichon, X., Bergerat, F. and Roulet, M.J., 1988. Plate kinematics and tectonics leading to Alpine belt formation: a new analysis. In: Processes in Continental Lithospheric Deformation. Geol. Soc. Am., Spec. Pap., 218: 111–131.

Letouzey, J., 1986. Cenozoic paleo-stress pattern in the Alpine foreland and structural interpretation in a platform basin. Tectonophysics, 132: 215–231.

Letouzey, J. and Trémolieres, P., 1980. Paleo-stress fields around the Mediterranean since the Mesozoic derided from microtectonics: comparisons with plate tectonic data. In: Géologie des Chaines Alpines Issues de la Téthys. Int. Geol. Congr., 26th, Paris. Mém. Bur. Rech. Géol. Min., 115: 261–273.

Mattauer, M. and Mercier, J.L., 1980. Microtectonique et grande tectonique. Mem. Hors Sér. Soc. Géol. Fr., 10: 141–161.

Olsson, W.A., 1974. Grain size dependance of yield stress in marble. J. Geophys. Res., 79: 4859–4862.

Rat, P., 1976. Structures et phases de structuration dans les plateaux bourguignons et le Nord-Ouest du fossé bressan (France). Geol. Rundsch., 65: 101–126.

Rowe, K.J. and Rutter, E.H., 1990. Paleostress estimation using calcite twinning: experimental calibration and application to nature. J. Struct. Geol., 12 (1): 1–17.

Savostin, L.A., Sibuet, J.C., Zonenshain, L.P., Le Pichon, X. and Roulet, M.J., 1986. Kinematic evolution of the Tethys belt from the Atlantic ocean to the Pamirs since the Triassic. Tectonophysics, 123: 1–35.

Tourneret, Ch., 1987. Détermination du tenseur des contraintes tectoniques par les macles de la calcite. Mise au point d'une méthode automatique de mesures. Unpublished D.E.A, Univ. Sciences et Techniques du Languedoc, Montpellier, 50 pp.

Tourneret, Ch. and Laurent, Ph., 1990. Paleostress orientations from calcite twins in the North Pyrenean foreland, determined by the Etchecopar inverse method. Tectonophysics, 180: 287–302.

Tullis, T.E., 1980. The use of mechanical twinning in minerals as a measure of shear stress magnitudes. J. Geophys. Res., 85: 6263–6268.

Turner, F.J., Griggs, D.T. and Heard, H., 1954. Experimental deformation of calcite crystals. Geol. Soc. Am. Bull., 65: 883–934.

Villemin, T., 1986. Tectoniques en extension, subsidence et fracturation: le fossé rhénan et le bassin sarro-lorrain. Thèse de Doctorat, Mém. Sci. Terre Univ. P. et M. Curie, no. 86-01 Paris, 270 pp.